JMSR 1(3) (2025)

Journal of Material Science and Radiation

https://journals.balaipublikasi.id/jmsr

Effect of Gamma Irradiation on the Optical Characteristics of PVA-PANI Composite Polymer Films

Norfazlinayati Othman[1], Mohd Hamzah Harun[2*], Mahathir Mohamed[2], Mohd Sofian Alias[2], Zainal Abidin Talib[3]

[1] Department of Physics, Faculty of Science, Universiti Putra Malaysia, 43400, Serdang, Selangor, Malaysia
[2] Radiation Processing Technology Division, Malaysian Nuclear Agency, Bangi, 43000, Kajang, Selangor, Malaysia
[3] Department of Physics, College of Natural Sciences, Jeonbuk National University 567, Baekje-daero, Deokjin-gu, Jeonju-si, Jeollabuk-do, 54896 Republic of Korea

Received: June 3, 2025
Revised: September 30, 2025
Accepted: December 25, 2025
Published: December 31, 2025

Corresponding Author:
Mohd Hamzah Harun
hamzah@nm.gov.my

DOI: 10.56566/jmsr.v1i3.394

Abstract: This manuscript reports the optical and structural characteristics of PVA/PANI composite polymer films synthesized through gamma-irradiation-induced in-situ polymerization. The in-situ formation of the conductive emeraldine salt phase of polyaniline (PANI) within the polyvinyl alcohol (PVA) binder matrix was achieved under different irradiation doses. The formation of the conductive PANI phase and the presence of Cl^- counter-ions were confirmed through FESEM morphological analysis and EDAX elemental mapping, respectively. XRD spectra further verify the semi-crystalline nature of the composite and indicate the structural role of PVA as a binder in stabilizing the polymeric composite system. Thermal behavior analysis using TGA reveals four distinct decomposition phases, with the most pronounced thermal transition observed in the composite irradiated at 50 kGy, suggesting enhanced structural interactions between PVA and PANI at this irradiation dose. Overall, the results demonstrate that gamma irradiation is an effective route for modifying the optical, structural, and thermal properties of PVA/PANI composites, making them promising candidates for optoelectronic and conductive polymer applications.

Keywords: Gamma irradiation; PVA/PANI; Optical characteristic

Introduction

Gamma radiation has emerged as a powerful and versatile tool in the field of material science, owing to its ability to induce significant modifications in the physical, chemical, and structural properties of materials without the need for conventional thermal or chemical processing (Naikwadi et al., 2022). As a form of high-energy electromagnetic radiation, gamma rays possess deep penetration capability and sufficient energy to break chemical bonds, thereby generating reactive species such as free radicals within the polymer matrix. These reactive species can initiate polymerization, crosslinking, or chain scission processes depending on the nature of the material and the irradiation conditions applied. Globally, the utilization of gamma irradiation has expanded across various industrial and research sectors due to its distinct advantages—clean processing, minimal contamination, and precise control over reaction kinetics.

In particular, gamma radiation is increasingly used in the synthesis and modification of conductive polymers, such as polyaniline (PANI), due to its ability to facilitate in-situ polymerization under mild conditions (MacDiarmid, 2001). Unlike traditional chemical polymerization methods that require strong oxidizing agents, acidic dopants, or surfactants, the gamma irradiation approach provides an eco-friendly alternative by eliminating the use of potentially hazardous reagents (Patil et al., 2011; Deshmukh et al., 2015). This technique enables the direct formation of conducting polymer chains through the radiation-induced generation of active sites, enhancing both the efficiency and purity of the polymerization process (Clough, 2001). When applied to conductive polymers, gamma irradiation not only initiates the polymerization of monomers such as anilinium hydrochloride (AniHCl) but also influences the resultant material's microstructure and morphology.

The energy deposited by gamma rays can promote the alignment and ordering of polymer chains, leading

How to Cite:
Othman, N., Harun, M. H., Mohamed, M., Alias, M. S., & Talib, Z. A. Effect of Gamma Irradiation on the Optical Characteristics of PVA-PANI Composite Polymer Films. *Journal of Material Science and Radiation*, *1*(3), 76–82. https://doi.org/10.56566/jmsr.v1i3.394

to improved crystallinity, enhanced electrical conductivity, and better thermal stability. Additionally, gamma irradiation can assist in achieving a more homogeneous dispersion of the conducting polymer within composite matrices, such as polyvinyl alcohol (PVA), thus improving interfacial adhesion and overall mechanical integrity (Othman et al., 2018). Numerous studies have demonstrated that the structural characteristics of gamma-irradiated PANI and PANI-based composites exhibit superior performance compared to those synthesized via conventional routes. For example, irradiation-induced polymerization of PANI has been reported to yield materials with higher degrees of protonation, more defined morphological features (such as nanofiber or granular structures), and improved electrochemical behavior—features that are crucial for applications in flexible electronics, sensors, supercapacitors, and electromagnetic shielding materials (Othman et al., 2018).

In this context, the present work explores the application of gamma irradiation in the synthesis of PANI and its composites, focusing on how varying irradiation doses influence the structural, thermal, and morphological properties of the resulting materials. By understanding the underlying mechanisms of radiation-induced polymerization and its effects on material characteristics, this study aims to establish gamma irradiation as a reliable, green, and effective technique for developing high-performance conductive polymer composites.

Method

The PVA/PANI composite film was prepared by dissolving 75 parts per hundred (pph) (0.9 g) of aniline hydrochloride (AniHCl) monomer (Aldrich)into 40 mL of a PVA (98%, Merck) stock solution. The mixture was stirred using a conventional magnetic stirrer for 2 hours to ensure homogeneity. The resulting solution was then poured into a 9 cm diameter glass Petri dish and dried in an oven at 48–51 °C for 48 hours. After the film was peeled from the Petri dish, it was subjected to γ-irradiation at doses of 10, 20, 30, 40, and 50 kGy, conducted at the Unit Sinagama, Malaysian Nuclear Agency, Bangi. The average thickness of the films was measured using a digital micrometer (Mitutoyo, model: 486-8210) and found to be t = 0.16 ± 0.02 mm**.**

Result and Discussion

FESEM and EDAX Analysis

The surface morphology of the PVA/PANI composite film was examined using Field Emission Scanning Electron Microscopy (FESEM) and Energy Dispersive X-ray Analysis (EDAX), as presented in Figure 1.

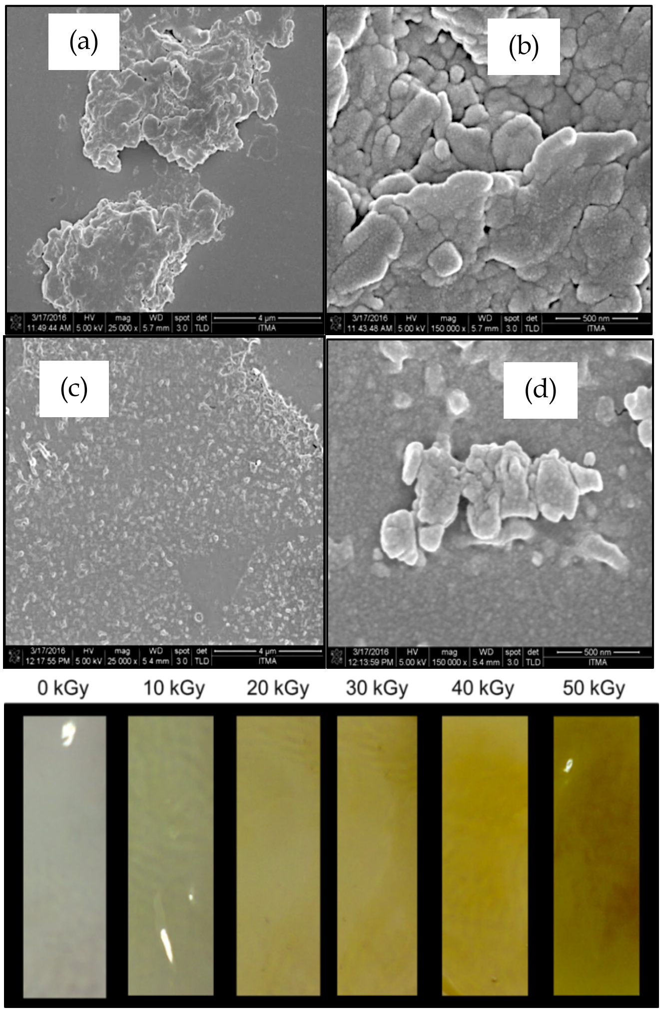

Figure 1: FESEM micrograph of PVA/PANI composite film (a) before (mag. 25k x), (b) before (mag.150k x), (c) after irradiation at 50 kGy (mag. 25k x), (d) after irradiation at 50 kGy (mag. 150k x) and (e) The response of PVA film and 75pph of PVA/PANI composite film after being exposed to γ-irradiation.

The results clearly indicate that Figure 1(a), which shows the surface of the PVA/AniHCl composite film, exhibits a nonhomogeneous structure. This irregular morphology is attributed to the presence of protonated aniline grains, which are embedded and distributed throughout the PVA matrix. The average grain size is estimated to be below 500 nm, based on measurements obtained from the Nova NanoSEM 230 operating system. The morphological structure, however, changed after irradiation. Radiation led to the formation of small clusters with an oblong, rod-like shape that were uniformly distributed across the film surface, as shown in Figure 1(c) and (d). The uniform dispersion of the polymer within the PVA matrix is confirmed by the green color, which appears homogeneous throughout the film (Figure 1(e)).

The color of the film darkens to a deeper green as the irradiation dose increases, indicating that the polymer is in the emeraldine salt (ES) form. According to Bhat et al. (2008), such color changes and the emergence of oblong shapes occur when the polymers become conductive. In this case, PANI becomes conductive after being doped with Cl^- anions, which act as oxidizing agents during the polymerization process initiated by γ-radiation. The presence of Cl^- ions in the film is supported by EDAX results (Figure 2(a) and (b)). The weight percentage of Cl^- decreased by 26.6%, from 31.75 wt% in the unirradiated film to 5.15 wt% in the irradiated film. This suggests that Cl^- ions are dispersed across the film surface during the polymerization process. The mechanism of the polymerization process can be explained by analogy to conventional chemical doping. In typical chemical polymerization, if oxidation begins under alkaline conditions, aniline oligomers are produced, turning the reaction mixture brown and making it insoluble in water (Deshmukh et al., 2015). This results in the formation of non-conductive PANI (Konyushenko et al., 2006). In contrast, when oxidation occurs in a highly acidic environment, the brown oligomers are scarcely observed due to their low concentration. Instead, a blue color appears, which is attributed to the initial oxidation of aniline and the early growth of PANI chains—this intermediate form is commonly referred to as emeraldine base (EB-PANI). Upon completion of the polymerization process, PANI transforms into a green or dark green homogeneous mixture, depending on the concentration of oxidizing agents and dopants used during synthesis. This final form is known as emeraldine salt (ES-PANI) (Sevil et al., 2000).

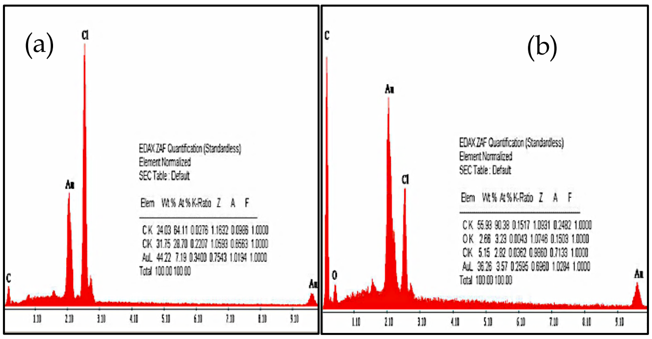

```
EDAX ZAF Quantification (Standardless)
Element Normalized
SEC Table : Default

Elem  Wt %  At % K-Ratio  Z      A      F
C K   24.03 64.11 0.0276 1.1632 0.0986 1.0000
ClK   31.75 28.70 0.2207 1.0593 0.6563 1.0000
AuL   44.22  7.19 0.3400 0.7543 1.0194 1.0000
Total 100.00 100.00
```

```
EDAX ZAF Quantification (Standardless)
Element Normalized
SEC Table : Default

Elem  Wt %  At % K-Ratio  Z      A      F
C K   55.93 90.38 0.1517 1.0931 0.2482 1.0000
O K    2.66  3.23 0.0043 1.0746 0.1503 1.0000
ClK    5.15  2.82 0.0362 0.9860 0.7133 1.0000
AuL   36.26  3.57 0.2595 0.6960 1.0284 1.0000
Total 100.00 100.00
```

Figure 2. EDX spectra of PVA/Aniline hydrochloride composites film for (a) before and (b) after irradiation at 50 kGy

From this perspective, a similar approach can be applied to the synthesis of PANI via γ-irradiation. However, it should be noted that controlling the conditions of irradiation is significantly more complex than in conventional methods (Bodugöz & Güven, 2005). γ-irradiation may also lead to side reactions and the formation of by-products. The process generates reactive sites on aniline monomers and hydrochloric acid (HCl), facilitating the propagation of the reaction through mechanisms such as Compton scattering or the photoelectric effect. The energy from γ-rays can break weak bonds in the aniline monomer ring; particularly the $-NH_3^+$ group—allowing doping with Cl^- ions and forming PANI dimers.

This process is known as in-situ polymerization (Sharma et al., 2014). It occurs rapidly and continuously during irradiation, eventually resulting in the formation of a complete polymer backbone. A proposed reaction mechanism for PANI synthesis via γ-irradiation is illustrated in Figure 3.

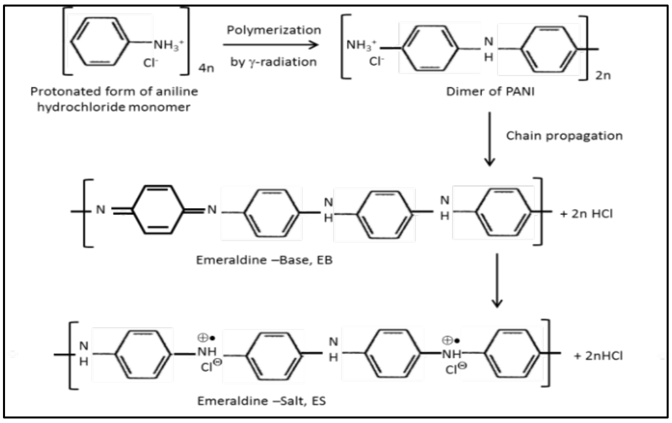

Figure 3. Schematic of possible reaction polymerization mechanism of PANI via γ-irradiation

XRD Analysis

The structural characteristics of the PVA/PANI composite film, before and after exposure to γ-radiation, were analyzed using XRD spectroscopy. Figure 3 presents the XRD patterns of PVA/PANI composite films irradiated at various γ-ray doses. In the as-synthesized (0 kGy) PVA/PANI film, diffraction peaks appear at 2θ values of 21.1°, 21.9°, 22.7°, and 35.6°. The main diffraction peak centered at 2θ = 21°, corresponding to the (100) plane, is attributed to the periodicity parallel to the PANI chains. Additionally, the broad peak at 2θ = 19.2° represents the characteristic amorphous peak of PVA (Nguyen & Shim, 2015). Following irradiation, the PVA peak shifts slightly to a higher angle—from 19.2° at 0 kGy to 20.2° at 30 kGy. This shift indicates distortion in the polymer plane and a reduction in interplanar spacing, as summarized in Table 1. This effect is likely due to interactions between the PANI and PVA chains during the polymerization process. It is believed that aniline hydrochloride within the PVA matrix enhances crosslinking of the PVA chains by PANI, which introduces strain along the polymer backbone (Mahmoud et al., 2012). Interestingly, at higher doses (40 and 50 kGy), the diffraction peaks shift back toward their original positions, and additional new peaks emerge. This reversal may indicate a reduction in crosslinking activity, possibly because the PANI monomers have been fully polymerized, minimizing further interaction with the PVA chains (Bhat et al., 2008). These observations suggest that PVA effectively serves as a binder in the composite film, maintaining structural integrity even after high-dose irradiation (Harun et al., 2019).

The main diffraction peak of PANI, centered at 2θ = 21°, shifted toward higher angles after irradiation at 10, 20, and 30 kGy. This shift is attributed to the reciprocal interaction with PVA chains. At higher doses (40 and 50 kGy), the peak returns to its original position, as shown in Figure 4. Notably, increasing the irradiation dose also enhances the crystallinity of PANI. At 40 kGy, new diffraction peaks emerge at 2θ = 23°, and at 50 kGy, all characteristic crystalline peaks of PANI become clearly visible in the 2θ range of 21° to 35°. The increase in crystalline peaks is supported by changes in the interlayer spacing.

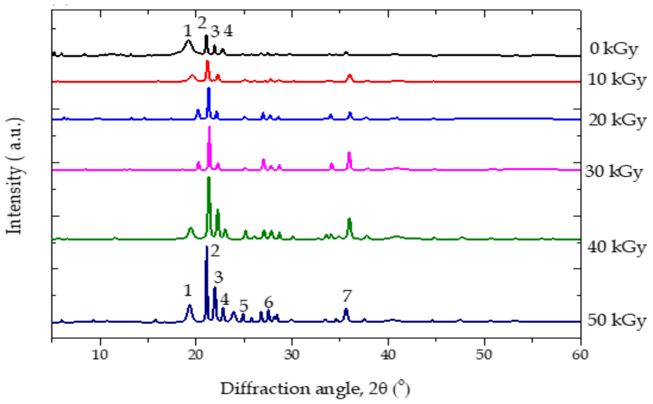

Figure 3. XRD pattern of PVA/PANI composite films at different doses

Table 1. XRD analysis of PVA/PANI composite film

PVA/ PANI film [kGy]	Peak no.	Peak pos. [°2Th]	d-spacing [Å]	FWHM [°]	Crystallite size, L [nm]	Lattice strain [%]	Interlayer separation, S [Å]
0	1	19.2	4.62	0.78	11.1	2.01	5.77
	2	21.06	4.22	0.16	73.5	0.36	8.69
	3	21.9	4.05	0.13	101.1	0.27	5.07
	4	22.76	3.9	0.26	38.6	0.55	4.88
	5	-	-	-	-	-	-
	6	-	-	-	-	-	-
	7	35.58	2.52	0.26	39.7	0.345	3.15
10	1	19.58	4.53	0.65	13.5	1.64	5.66
	2	21.26	4.14	0.23	45.7	0.51	5.18
	3	22.26	3.99	0.26	38.6	0.57	4.99
	4	-	-	-	-	-	-
	5	-	-	-	-	-	-
	6	-	-	-	-	-	-
	7	35.95	2.5	0.39	24.6	0.52	3.12
20	1	19.99	4.39	0.26	38.4	0.63	5.49
	2	21.37	4.17	0.16	72.2	0.36	5.21
	3	22.12	4.02	0.16	72.3	0.34	5.02
	4	-	-	-	-	-	-
	5	-	-	-	-	-	-
	6	27.51	3.24	0.16	73	0.28	4.05
	7	36	2.49	0.2	57.6	0.25	3.12
30	1	20.01	4.39	0.16	72.1	0.38	5.48
	2	21.45	4.16	0.13	101.1	0.28	5.20
	3	22.25	3.99	0.23	45.7	0.49	4.99
	4	-	-	-	-	-	-
	5	-	-	-	-	-	-
	6	26.95	3.31	0.13	102.1	0.22	4.13
	7	35.91	2.5	0.2	57.6	0.25	3.12
40	1	19.43	4.56	0.52	17.1	1.32	5.71
	2	21.39	4.16	0.23	45.7	0.51	5.21
	3	22.23	3.99	0.23	45.7	0.49	4.99
	4	-	-	-	-	-	-
	5	23.02	3.89	0.26	38.6	0.55	4.82
	6	27.05	3.29	0.26	38.9	0.46	4.12
	7	35.93	2.49	0.29	34.5	0.39	3.12
50	1	19.32	4.59	0.52	17.1	1.33	5.74
	2	21.09	4.21	0.13	101	0.28	5.26
	3	21.95	4.05	0.23	45.7	0.5	8.35
	4	22.79	3.9	0.2	55.9	0.41	4.87
	5	23.88	3.72	0.42	21.8	0.87	4.65
	6	27.51	3.24	0.16	73	0.28	4.05
	7	35.58	2.52	0.33	30.3	0.44	3.15

Upon irradiation at 10 kGy, the interlayer distance decreases from 8.69 Å to 5.18 Å, as shown in Table 1. This reduction indicates that the polymer chains in the composite film become more compact and well-aligned after irradiation. However, with further increases in dose, the interlayer distance slightly increases—from 5.18 Å at 10 kGy to 5.26 Å at 50 kGy—suggesting a structural response to the polymerization process initiated by γ-radiation. During this polymerization, defects form in the structure, resulting in quasi-particles known as polarons and bipolarons. These provide pathways for electron transport. As the irradiation dose increases, more polarons and bipolarons are generated, leading to a higher degree of structural defects. These defects contribute to increased disorder within the polymer structure, which in turn causes a slight increase in interchain layer separation (Bhadra & Khastgir, 2008).

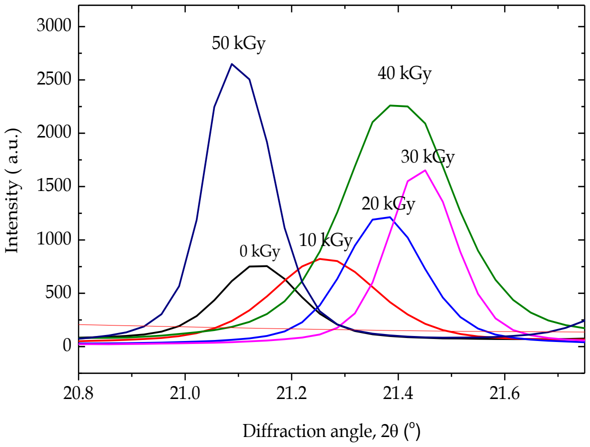

Figure 4. XRD pattern of PVA/PANI composite film irradiated at 0 to 50 kGy by γ-rays

Based on the observed data and the shift in diffraction peaks discussed earlier, it can be inferred that at lower irradiation doses, the yield of polymerization is relatively low. As the dose increases, more energy is available to initiate polymer chain formation, leading to a higher yield of polymerization. This is consistent with the increased crystallinity and the emergence of distinct PANI peaks at higher doses, as described in the previous section. The trend is analogous to conventional chemical polymerization, where increasing the concentration of the oxidizing agent results in a higher polymerization yield. Therefore, as supported by the changes in interlayer spacing and crystallinity observed in the XRD analysis, it can be concluded that optimal polymerization of the emeraldine salt (ES) form of PANI occurs at 50 kGy. At this dose, all characteristic PANI peaks are distinctly visible, in agreement with previously reported studies (Geethalakshmi et al., 2016). This confirms that the γ-radiation-induced polymerization process effectively enhances the structural order and possibly, the conductivity of the PVA/PANI composite film.

TGA Analysis

Figure 5 shows the TGA thermogram for PVA/PANI composite films at different irradiation dose. The composite shows four decomposition phases in which the first region is at 100 – 150 °C. The second phase occurs at 150 - 208 °C. The third one is at 300 - 437 °C and the final phase is at 500 - 700 °C. The thermogram of PVA/PANI composite film is slightly different in which the typical decomposition phase of PVA (Jia et al., 2015). One of the reasons is due to the radiation polymerization of PANI that is formed after AniHCl is polymerized with the presence of gamma irradiation. The first phase is due to water based weight loss stage in which it is attributed to the bonding and deionized water presence in the intermolecular structure of the composite right after the temperature is above 100 °C (Tsioptsias & Zacharis, 2024).

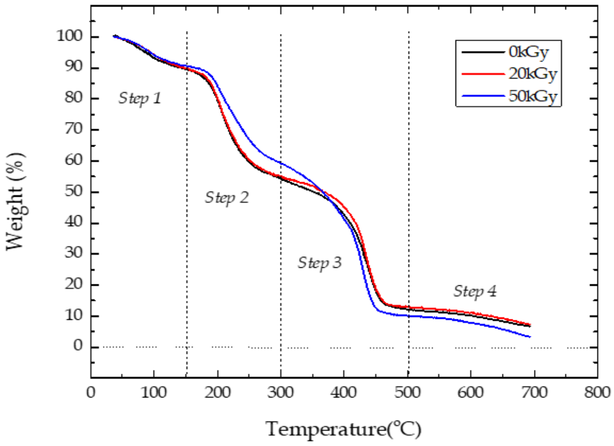

Figure 5. TGA thermogram for PVA/PANI composite films irradiated at 0, 20 and 50 kGy

The second decomposition phase is attributed to the thermal degradation of PVA, specifically the breakdown of its side chains. Notably, the thermogram of the sample irradiated at 50 kGy exhibits a more pronounced curve compared to the others, indicating a higher content of PANI within the PVA matrix. This greater PANI presence enhances the thermal stability of the composite, as reflected in the broader decomposition range. The third phase primarily corresponds to the degradation of PANI, particularly the deprotonation of Cl^- dopants present in the PVA/PANI composite films (Nguyen & Shim, 2015). As the temperature approaches 400 °C, increased polymer chain mobility leads to the release of gases such as NH_3 and CO_2, which contribute significantly to the mass loss observed during this stage.

Table 2. TGA data for PVA/PANI composite film irradiated at 0, 20 and 50 kGy

γ-ray dose (kGy)	*Step 1* *(Below 150 ℃)* Weight loss (%)	*Step 2* *(150-300 ℃)* Weight loss (%)	*Step 3* *(300-500 ℃)* Weight loss (%)	*Step 4* *(500-700 ℃)* Weight loss (%)	Total weight loss (%)
0	T_{max}= 87.18^{0}C 10.10	T_{max}= 208.79^{0}C 36.02	T_{max}= 437.13^{0}C 42.18	T_{max}= 700^{0}C 5.01	93.31
20	T_{max}= 97.57^{0}C 10.10	T_{max}= 205.74^{0}C 35.47	T_{max}= 434.08^{0}C 41.48	T_{max}= 700^{0}C 5.57	92.62
50	T_{max}= 93.09^{0}C 9.82	T_{max}= 207.17^{0}C 30.16	T_{max}= 428.17^{0}C 50.24	T_{max}= 700^{0}C 6.47	96.69

The final phase, often referred to as the carbonization stage, occurs at approximately 500 °C. At this temperature, the main polymer backbones within the composite are fully decomposed, resulting in the formation of a carbonaceous residue. Beyond this point, further increases in temperature have minimal impact on the mass loss, indicating that the majority of volatile components have already been eliminated (Wang et al., 2012). Table 2 summarizes the TGA and DTG data, detailing the degradation phases of the PVA/PANI composite films at different irradiation doses, along with the corresponding weight loss observed in each stage.

Conclusion

In summary, the optical properties of PVA/PANI composite films induced by gamma irradiation have been investigated. FESEM micrograph confirms the PANI formation upon irradiation of AniHCl in the PVA binder whereas EDAX indicates the presence of Cl- anion in the composite polymer. This anion is responsible to the formation of polaron within the PANI structure. XRD spectra indicates the role of PVA as a binder in the composite polymer. The reduction of interlayer distance suggests that the polymer system becomes more compact and more align due to the reaction with irradiation doses. The TGA themogram shows that the PVA/PANI composite polymer experienced four decomposition phases. At 50 kGy, a more pronounced curve compared to the others is observed due to the higher content of PANI within the PVA matrix.

Acknowledgements
The authors thank to UPM for the financial support. The technical assistance from MTEG lab and gamma irradiation facility from Malaysian Nuclear Agency are highly appreciated.

Author Contributions

Conceptualization, Z. A. T. and N. O; methodology, software, N. O and M. H. H.; validation, M. M. and M. S. A; formal analysis, N. O. and Z. A. T.; investigation, N. O., M. H. H. and Z. A. T.; resources, Z. A. T.; data curation, N. O. and Z. A. T; writing—original draft preparation N. O. and M. H. H.; writing—review and editing, Z. A. T.; supervision, M. H. H and Z. A. T.; project administration, N. O. and Z. A. T.; funding acquisition, Z. A. T. All authors have read and agreed to the published version of the manuscript.

Funding
This research was funded by GP-IPB grant under UPM.

Conflicts of Interest
The authors declare no conflict of interest.

References

Bhadra, S., & Khastgir, D. (2008). Determination of crystal structure of polyaniline and substituted polyanilines through powder X-ray diffraction analysis. *Polymer Testing*, 27(7), 851–857. https://doi.org/10.1016/j.polymertesting.2008.07.002

Bhat N.V., Nate M.M., Gore A. V., & Bhat R.M. (2008). Interaction of Gamma Radiation with PVA/PANi Composite Films: Structural and Morphological Studies. *Journal of Applied Polymer Science*, 110, 2243–2252. https://doi.org/10.1002/app.28641

Bodugöz, H., & Güven, O. (2005). Radiation induced dehydrochlorination as an in-situ doping technique for enhancement of the conductivity of polyaniline blends. *Nuclear Instruments and Methods in Physics Research, Section B: Beam Interactions with Materials and Atoms*, 236(1–4), 153–159. https://doi.org/10.1016/j.nimb.2005.04.009

Clough, R. L. (2001). High-energy radiation and polymers: A review of commercial processes and emerging applications. *Nuclear Instruments and Methods in Physics Research Section B: Beam Interactions with Materials and Atoms*, 185(1-4), 8-33. https://doi.org/10.1016/S0168-583X(01)00966-1

Deshmukh, P. R., Patil, S. V., Bulakhe, R. N., Pusawale, S. N., Shim, J. J., & Lokhande, C. D. (2015). Chemical synthesis of PANI–TiO 2 composite thin film for supercapacitor application. *RSC Advances*, 5(84), 68939-68946. https://doi.org/10.1039/C5RA09233G

Geethalakshmi, D., Muthukumarasamy, N., & Balasundaraprabhu, R. (2016). Measurement on the structural, morphological, electrical and optical properties of PANI-CSA nanofilms. *Journal of the International Measurement Confederation*, 92, 446–452. https://doi.org/10.1016/j.measurement.2016.06.054

Harun, M. H., Othman, N., Mohamed, M., Alias, M. S., Umar, K. N., & Rahman, M. F. (2019). Influence of gamma irradiation on the electrical conductivity and dielectric properties of polypyrrole conducting polymer composite films. *International Journal of Nanoelectronic and Materials*, 12(4), 467-476. Retrieved from http://dspace.unimap.edu.my/xmlui/handle/123456789/62488

Jia, P., Zhang, M., Bo, C., Hu, L., & Zhou, Y. (2015). The plasticizing effect of properties of manganous chloride and glycerin on poly (vinyl alcohol). *Polish Journal of Chemical Technology,* 17(2). https://doi.org/10.1515/pjct-2015-0025

Konyushenko, E. N., Stejskal, J., Trchová, M., Hradil, J., Kovářová, J., Prokeš, J., Sapurina, I. (2006). Multi-wall carbon nanotubes coated with polyaniline. *Polymer*, 47(16), 5715–5723. https://doi.org/10.1016/j.polymer.2006.05.059

MacDiarmid, A. G. (2001). Nobel Lecture: "Synthetic metals": A novel role for organic polymers. *Reviews of Modern Physics,* 73(3), 701–712. https://doi.org/10.1002/1521-3773(20010716)40:14%3C2581::AID-ANIE2581%3E3.0.CO;2-2

Mahmoud, W. E., Al-Ghamdi, A. A., & Kadi, M. W. (2012). The influence of γ-rays irradiation on the structure and crystallinity of heteropoly acid doped PVA. *Radiation Physics and Chemistry*, 81(6), 693–696. https://doi.org/10.1016/j.radphyschem.2012.02.009

Naikwadi, A. T., Sharma, B. K., Bhatt, K. D., & Mahanwar, P. A. (2022). Gamma radiation processed polymeric materials for high performance applications: a review. *Frontiers in Chemistry*, 10, 837111. https://doi.org/10.3389/fchem.2022.837111

Nguyen, V. H., & Shim, J.-J. (2015). Green Synthesis and Characterization of Carbon Nanotubes/Polyaniline Nanocomposites. *Journal of Spectroscopy*, 2015, 1–9. https://doi.org/10.1155/2015/297804

Othman N., Talib, Z. A., Nik Salleh, N. G., Shaari, A. H., & Mohd Hamzah, H. (2018). Synthesis and Characterization of Polyvinyl alcohol/Polyaniline/Functionalized Multiwalled Carbon Nanotube Composite by Gamma Radiation Method. *International Journal of Nanoelectronics & Materials*, 11(4).

Patil, D. S., Shaikh, J. S., Dalavi, D. S., Kalagi, S. S., & Patil, P. S. (2011). Chemical synthesis of highly stable PVA/PANI films for supercapacitor application. *Materials Chemistry and Physics*, 128(3), 449-455. https://doi.org/10.1016/j.matchemphys.2011.03.029

Sevil, U. A., Guven, O., Birer O., & Suzer S. (2000). Doping of 2-Cl-PANI/PVC films by exposure to UV, Gamma rays and e-beams, *Synthetic Metals*, 110, 175-179. https://doi.org/10.1016/S0379-6779(99)00266-0

Sharma, K., Kaith, B. S., Kumar, V., Kalia, S., Kumar, V., & Swart, H. C. (2014). Synthesis and biodegradation studies of gamma irradiated electrically conductive hydrogels. *Polymer Degradation and Stability*, 107, 166–177. https://doi.org/10.1016/j.polymdegradstab.2014.05.014

Tsioptsias, C., & Zacharis, A. K. (2024). Simulation and Experimental Study of the Isothermal Thermogravimetric Analysis and the Apparent Alterations of the Thermal Stability of Composite Polymers. *Polymers,* 16(11), 1454. https://doi.org/10.3390/polym16111454

Wang, Q., Yao, Q., Chang, J., & Chen, L. (2012). Enhanced thermoelectric properties of CNT/PANI composite nanofibers by highly orienting the arrangement of polymer chains. *Journal of Materials Chemistry*, 22(34), 17612–17618. https://doi.org/10.1039/C2JM32750C